Effects of Differently Incubated Cupric Oxide Nanoparticles on the Granulosa Cells of Caprine Ovary *in Vitro*

Chetan Kumar
Kurukshetra University Department of Zoology
Rajnesh Kumar Sharma (rksharmakukz@gmail.com)
Kurukshetra University Department of Zoology https://orcid.org/0000-0002-7975-6382

Research Article

Keywords: Cupric Oxide Nanoparticles, Cytotoxicity, Granulosa cells, XRD, FTIR, HRTEM, FESEM, Temperature. antibiotic resistance

Posted Date: December 13th, 2021

DOI: https://doi.org/10.21203/rs.3.rs-938179/v1

Abstract

Present study was aimed to investigate the effect of temperature on the shape and size of nanoparticles and related cytotoxicity of these particles on ovarian granulosa cells. Cupric oxide nanoparticles (CuONPs) were synthesized using a simple, efficient, and reproducible precipitation method involving reduction of Cu metal salt with sodium hydroxide and then incubation of the precipitates at 70^{o}C for 5 hrs. Subsequently, this prepared sample was divided into 3 subsamples and incubated at 3 different temperatures i.e. 70^{o}C, 150^{o}C, and 350^{o}C for a time duration of 5 hrs. to study the effect of temperature on the particles. The products were characterized by XRD, FTIR, HRTEM, and FESEM. Characterization of the particles revealed that all particles were monoclinic crystalline in nature and had a size range from 9 nm - 60 nm. Particles were of different shapes; spherical, needle, and capsule. Toxicity of each particle was determined on granulosa cells by exposing them for 24 hrs. at 2 different doses. Toxicological results showed the size and shape-related toxicity of nanoparticles; particles which were spherical shape were significantly more toxic than capsule-shaped particles.

Introduction

Nanomaterials are compounds and substances having a size range from 1nm to 100 nm in any one dimension (Buzea et al. 2007). In recent times these materials had played an important role in our ever-continuous quest to improve the quality of human life. The global nanotechnology market is expected to exceed the US$ 125 Billion mark by 2024 (Liu and Xia 2020). Nanoparticles differ from their bulk particles by thermal, mechanical, magnetic, electrical, and optical properties (Buzea et al. 2007). The nanoparticles have many applications in the field of chemical, physical, biological, engineering, material sciences as well as in electronic science (Ingale 2013). Among various nanotypes, metal oxides are of great interest because of their various applications in energy production and storage, sensors, nanoelectronics, cosmetics, water purification, drug delivery, and coolant (Ahamed et al. 2010, 2014). There are various methods to synthesize them; sol-gel method, precipitation method, vapours method, ball milling method, etc. (Tamilvanan et al. 2014). Due to the availability of vast applications and different methods of synthesis, research agencies, government, and even universities are interested to analyse the fate, benefits, toxicity, direct and indirect effects of metal oxide nanoparticles or nanoparticles containing products (Tang et al. 2015; Taghavi et al. 2013).

Oxides of transition metals are an important class of semiconductors and are used very commonly. Among other transition metals, copper is a good conductor and does not react with water (Cardeilhac and Whitaker 1988). It is one of the elements that are essential to humans. Copper plays some important roles like oxygen carrier and oxidation catalyst (2nd only to iron), it is also present in many proteins like hemocyanin, ceruloplasmin, monoamine oxidase, galactose oxidase, dopamine β-hydroxylase, superoxide dismutase, and phenolase (Richardson 1997). Copper compounds have many other roles like fungicide, bactericide, algaecide and also have functional role in plant photosynthetic enzymes (Richardson 1997). Simplest among the family of copper nanoparticles, cupric oxide nanoparticles (CuONPs) are considered as one of the most bio-reactive metal oxide nanoparticles (Karlsson et al. 2008

and Lanone et al. 2009). These particles have various applications in veterinary medicines, nano purification of sperms, germicides, biocides, food safety, and in reversing antibiotic resistance (Hill and Li 2017). These are also useful in heat transfer fluids, solar energy, catalysis, conductive coating in lithium-ion batteries, additives in lubricants, coatings for plastics, and gas sensors (Aruoja et al. 2009; Gawande et al. 2016).

The cytotoxic effects of CuO nanoparticles vs bulk particles have been reported in mammalian cells like neuronal cells, lung epithelial cells, cardiac microvascular endothelial cells, and liver cells (Fahmy and Cormier 2009; Ahamed et al. 2010; Sun et al. 2011; Wang et al. 2011; Piret et al. 2012; Siddiqui *et al*. 2013; Xu et al. 2013). Berntsen et al. (2010) reported the impaired cell viability and decreased cell contractility in human airway smooth muscle cells on CuONPs exposure. A dose-dependent decrease in cell viability of the human pulmonary epithelial cells (A549) by CuONPs also had been reported by Ahamed et al. (2010). These studies highlighted the decrease in the size of the particles as the main reason for NPs induced cytotoxicity. But emerging studies find that size may not be the only critical factor responsible for it. The other critical factors that might contribute to cytotoxicity are: shape (Gratton et al. 2008), surface chemistry (Liu et al. 2010), and particles solubility (Studer et al. 2010; Franklin et al. 2007).

Ovarian granulosa cells play an important role in the growth and maturation of a follicle (Sharma 2000). The apoptosis of granulosa cells a fundamental biological process of programmed cell death that leads to atresia is (Yu et al. 2004) characterized by condensed cytoplasm, pyknotic nuclei, and hazy cytoplasm (Sharma 2000). In addition to endocrine factors various xenobiotics and toxic chemicals have been reported for inducing apoptosis in the granulosa cells (Yu et al. 2004; Lima-Verde et al. 2012). Nanoparticles like calcium phosphate and gold can induce apoptosis of granulosa cells (Liu et al. 2010; Stelzer and Hutz 2009).

It has been reported that physicochemical properties, bio-distribution, internalization, biological response, and even cytotoxicity of the particles are affected by the shape of the particles (Huang et al. 2010; Venkataraman et al. 2011). Pal *et al*. (2007) proved that silver nanoparticles with truncated triangular nanoplates showed a stronger biocidal action than spherical and rod-shaped nanoparticles. Stoehr *et al*. (2011) also described that wire-shaped silver nanoparticles caused decreased cell viability and increased Lactate Dehydrogenase (LDH) release for A549 cells, while no such effects were observed for spherical silver nanoparticles. As most of the toxicological studies focus on nano vs. bulk particles, little is known about the shape-related toxicity of the particles. Therefore, in this study, we have attempted to synthesize four differently shaped Cupric Oxide nanoparticles by varying the temperature of the reaction and find their relative toxicity on the caprine granulosa cells.

Materials And Methods

The chemicals and accessories were of analytical grade and were collected as per the requirements. Copper (II) acetate monohydrate [$Cu(CH_3COO)_2.H_2O$], glacial acetic acid (CH_3COOH), polyvinylpyrrolidone (PVP; MW 40,000), and culture media (DMEM) used were from HIMEDIA while sodium hydroxide pellets

(NaOH) used were from Rankem. Other chemicals were: Phosphate Buffer Saline (PBS), Deionized water (DI).

Apparatus & Instruments

Conical flasks, magnetic stirrer, funnel, the crucible, spatula, oven, furnace, burette and burette stand, CO_2 incubator, culture plates, fine forceps, needle, micropipettes, stereo-microscope, and fluorescent microscope.

Synthesis of Cupric Oxide NPs

Cupric Oxide Nanoparticles (CuONPs) were synthesized using the aqueous precipitation method (Ahamed *et al*. 2014), a type of chemical method which involves the reduction of a metal salt by reducing agent on the magnetic stirrer. In this method, 0.1 M of Copper (II) acetate monohydrate [$Cu(CH_3COO)_2.H_2O$)] was dissolved in deionized water to form an aqueous solution. This solution was reduced by another aqueous solution of NaOH drop by drop on a magnetic stirrer in a conical flask at the desired molar ratio of 1:10 under the glacial acetic acidic environment. PVP (Polyvinylpyrrolidone) was used as a stabilizer to control the growth of CuONPs' size and morphology. During the addition of the reducing agent, the color of the solution changed gradually from blue to sea green then from sea green to blackish-brown after which the reaction was stopped (Fig. 1). The blackish-brown solution indicates the synthesis of Cupric Oxide precipitates in solution. Obtained precipitates were washed with water and alcohol many times to remove the impurities present and dried at 70^oC for 5 hrs. (**T** Group). Particles were divided into 3 groups (**E1, E2,** and **E3)** and incubated at different conditions to know the effect of temperature at a constant time on the size and structure of nanoparticles (Table 1).

Collection of ovaries and culture of ovarian follicles in vitro

Ovaries of sexually mature, normal cycling Jamnapari breed of goat were brought to the lab in ice-cold 0.9% normal saline at 4oC from Municipal Slaughter House, Chandigarh (30^{o}70'N, 76^{o}80'S,). Follicles (3-8 mm diameter) from ovaries were manually separated using fine forceps and were classified as healthy, pre-atretic, and atretic follicles on the morphometric basis including vascularity, color, and turbidity of follicular fluid (Sharma and Bhardwaj 2009).

Healthy follicles (pinkish, highly vascularized having amber color follicular fluid) were cultured for 24 hrs. in 5 groups i.e. one control and 4 treatment groups (A, B, C, and D). Each treatment group was subdivided into 2 subgroups (1 and 2), where subgroup 1 had 10 µg ml^{-1} and 2 had 20 µg ml^{-1} concentration of respective CuONPs in culture media (Dulbecco's Modified Eagle Medium) supplemented with 200-units of antibiotics (100 IU/ml penicillin and 100 IU/ml streptomycin). These culture media were incubated in a CO_2 incubator (5% CO_2, 95% humidity, 38^oC temperature). The experimental layout of a follicular culture of goat ovaries is presented in Fig. 2.

Preparation of Granulosa Cell Suspension

The aspiration method was used to make cell suspension. Treated healthy follicles (3-8 mm) were aspirated with the help of a 20-gauge needle in a 2 ml syringe containing Phosphate Buffer Saline (PBS) at pH 7.4. Cumulus–Oocyte Complexes (COCs) were removed with the help of micropipettes under stereo-microscope. The remaining cell suspension was washed 3 times by centrifugation method with the help of (PBS) at 2000 rpm for 5 minutes each to remove any kind of debris.

Apoptotic assay

The morphometric analysis of the apoptotic granulosa cells was done by Broaddus *et al*. (1996) method. In this method granulosa cells' apoptosis was evaluated by Acridine Orange (AO) staining. Each cell suspension prepared from treated follicles was mixed with an equal quantity of AO solution. AO solution was made by dissolving 1 µL of AO in 1 ml PBS. Cells were then observed under fluoroscent microscope. Cells appearing green were normal, cells appearing yellow/orange were pre-apoptotic and cells which appeared red were apoptotic. Quantification of healthy, pre-apoptotic and apoptotic granulosa cells were done to measure Apoptotic Percentage Index (API).

Statistical analysis

Cytotoxicity data are expressed as mean±standard error. The cytotoxicity assay was analyzed with the help of One Way ANOVA with Tukey post-hoc test (all treatments were compared to control as well as to one other). For the statistical analysis, SPSS 16.0 was used. The p-values of less than 0.05 were considered significant.

Results

XRD

The X-Ray Diffraction (XRD) confirms the structural characterization of the particles. Samples were scanned in the range of 2θ from 10^o to 80^o by Panalytical's X'Pert Pro instrument with Ni filtered using CuKα radiations as an X-ray source (λ = 1.54060A$^\circ$). Peak analysis of the samples showed the reflecting planes of (110), ($\bar{1}$11), (111), ($\bar{2}$02), (020), (202), ($\bar{1}$13), ($\bar{3}$11), (220), (311) and (004) at 2θ; 32.3^o, 35.3^o, 38.5^o, 48.5^o, 53.3^o, 57.9^o, 61.2^o, 65.9^o, 67.7^o, 72.1^o and 74.9^o respectively (Fig. 3). The reflecting peaks of all the particles were in agreement with the NATIONAL BUREAU OF STANDARDS CIRCULAR (NBSC)-539 Volume-1 which concluded the presence of monoclinic structure. The absence of extra peak claims the purity of the substance. As shown in Fig. 3 major peaks appearing around 35^o and 38^o became longer and sharper as we go from T particles to E3 particles, thus the crystallinity order of these particles is E3 > E2 > E1 > T (Kulkarni 2015; Sedaghat et al. 2006).

The size of the particles using XRD can be evaluated by Debye-Scherrer equation.

$$T = \frac{k\lambda}{\beta \cos 2\theta}$$

Where,

T = Thickness of the crystal

k = Dimensionless shape factor, and its value is about 0.9

λ = Wavelength of the X-rays (1.5405A˚)

β = Broadening at half the maximum intensity (FWHM) caused by nanoparticle size

cos2θ = Angle between rays in beam and parallel planes (Bragg's angle)

Debye-Scherrer formula can be used to evaluate the average particle size smaller than 100 nm but larger than 2nm (Kulkarni 2015).

The crystal size of particle is given in Fig. 4.

FTIR

The Fourier Transmission Infrared Spectroscopic analysis of CuONPs describes the nature of bonds and types of functional groups present (Fig. 4). Identification of different functional groups and compounds is possible because different molecules absorb light of different energy in the infra-red region of the electromagnetic spectrum (Chopra et al. 2020). Transmittance bands present near the 500 cm-1 and 600 cm-1 wavelengths illustrate the presence of Cu-O bonds in samples, particularly Cu-O asymmetric stretching and Cu-O wagging respectively (Arun et al. 2015).

Figure 5 depicts that with a rise in temperature at constant time duration CuO bands became sharper and were of considerable depth. The bands present around 1630 cm-1 and 1380 cm-1 were may be due to M-O bond rocking in-plane (1383 cm -1) and M-O bond rocking out of the plane (1634 cm-1) attached as a bidentate ligand to the CuO (Arun et al. 2015). This presence of the carbonyl group may be due to the carbonyl group (= C = O) present in the pyrrolidone ring (Khan et al. 2020) or due to unreduced carboxyl group copper acetate or glacial acetic acid (Pal et al. 2015).

Whereas the absorbance bands present around 2920 cm^{-1} wavelength in the T, E1, E2 and E3 nanoparticles represented the asymmetric stretching of -CH_2- in the sample (Khan et al. 2020). An intense and broad absorbance band present at 3426 cm^{-1} (T), 3425 cm^{-1} (E1), 3417 cm^{-1} (E2), and 3354 cm^{-1} (E3) wavelength belonged to the stretching mode of hydroxyl group (-OH) of adsorbed water on the surface of CuONPs (Malviya et al. 2015). FTIR peaks have been summarised in Table 2.

FESEM

The effects of different incubation conditions on the morphology of CuONPs were studied by comparing the Field Emission Scanning Electron Microscopic images of different particles (Fig. 6). The T particles formed were spherical and aggregated to each other (Fig. 6a). The study of E1 particles found that the particles (Fig. 6b) were aggregated to each other and were trying to take needle-like shapes. But it was reversed in the case for E2 particles, (Fig. 6c) where the majority of particles were needle shape and fewer were aggregated. Finally, E3 particles obtained a capsule-like structure with definite boundaries and were well separated from each other (Fig. 6d).

HRTEM

The results of the High-Resolution Transmission Electron Micrograph (Fig. 7) of nanoparticles were in agreement with FESEM results. Where T particles were spherical (Fig. 7a) and aggregated with an average diameter of 9.42 ± 2.82 nm. With an increase in temperature E1 particles acquired a needle shape structure, uneven boundaries, and average diameter of 56.82 ± 13.61 nm (Fig. 7b). With further increase in temperature i.e. at 150^{o} C the E2 particles showed a diameter of 68.78 ± 18.55 nm and a shape intermediary of needle and capsule with uneven boundaries (Fig. 7c). While E3 particles were capsule shape (Fig. 7d) and showed a reverse trend i.e. size of the particles reduced with an average diameter of 41.62 ± 6.54 nm.

The size distribution pattern of all four types of particles can be seen in Fig. 8. The graphs show the particles are well distributed and size well below 100 nm. The peak of distribution in each nanoparticle matched the average size of the particles.

Frequency of Apoptosis

The Apoptotic Percentage Index (API) obtained by Fluorescent staining of granulosa cells with acridine orange showed the shape and dose-related toxicity of the CuONPs (Fig. 9). API depicts that there was an increase in the percentage of pre-apoptotic and apoptotic cells and a decrease in the percentage of healthy cells in all treatment groups as compared to control (Fig. 10). API also reported toxicity in higher dose groups compared to lower dose groups (Fig. 11).

While observing the significant difference in healthy cells the difference was reported only in the case of both doses of T nanoparticles and higher doses of E1, E2, and E3 nanoparticles compared to control. When we compared pre-apoptotic cells of treated and untreated cultural groups, it appeared that as compared to control all types of nanoparticles showed a significant increase in the percentage of pre-apoptotic cells except E3 nanoparticles at 10 µg ml^{-1} dose (Table 3) (Fig. 11). But when groups were observed for apoptosis, only those groups treated with higher dose i.e. 20 µg ml^{-1} showed a significant increase in the percentage of apoptotic cells as compared to control.

While comparing one nanoparticle to another nanoparticle, T nanoparticles at higher doses proved significantly more toxic than the rest of the three nanoparticles at 10 µg ml^{-1} doses when healthy cells

were observed. In the case of pre-apoptotic evaluation, a significant difference was observed only between T nanoparticles at 20 µg ml^{-1} and E3 nanoparticles at 10 µg ml^{-1}. Similarly, while observing all the treatment groups for apoptotic cells T nanoparticles with higher doses showed significant differences than lower doses of E1, E2, and E3 nanoparticles. While no other significant differences between nanoparticles were observed in the case of dose or types of nanoparticles.

Although when the lower dose of a nanoparticle was compared with the higher dose of the same nanoparticle none of the aforesaid particles showed any significant change in the number of cells either it was healthy cell count or pre-apoptotic cell count or it was apoptotic cell count. But all types of nanoparticles showed an increase in the percentage of apoptotic cells from lower dose to higher dose at 24 hrs. cultural duration.

Discussion

This study was conducted to examine the effects of the temperature variations on the size and shape of nanoparticles and the impact of differently sized and shaped nanoparticles on ovarian granulosa cells. CuONPs were synthesized by the precipitation method because this method provides better controllability and reproducibility of the nanoparticles, similar peculiarities were documented by Ficai and Grumezescu (2017) using the precipitation method. The effects of different temperature on size and shape CuONPs were evaluated by techniques like XRD, FTIR, FESEM, and HRTEM. XRD technique proved that all the particles formed were monoclinic crystals and had a size range from ~ 12 nm to ~ 14 nm. An increase in crystal size with the increase in temperature for T, E2, and E3 nanoparticles can be attributed to the phenomenon of “nuclear aggregation”. Nuclear aggregation is the phenomenon in which rapid formation of crystal nucleus and simultaneous aggregation of these nuclei occurs as the temperature rises. These findings strongly support the earlier findings of Vidyasagar et al. (2012). However, the decrease in E1 crystal size can be attributed to prolonged exposure of 70^{o}C temperature for 5 hrs. The nucleation rate for CuONPs remained constant, and thus crystal size did not increase rather it decreased because of the nucleation rate effect as already documented by Hongyu *et al*. (2020).

Morphological evaluation done by FESEM concluded that the shape of particles changed from spherical to capsule with the intermediary stages observed in E2 and E3 particles as the incubation conditions were changed. The FESEM analysis also found that different shapes of nanoparticles produced were actually due to the aggregation between spherical T nanoparticles. HRTEM analysis concluded that while the size of the particles increased up to 150^{o} C but then decreased. This reduction in the size of E3 nanoparticles compared to E2 and E1 nanoparticles can be attributed to the more evaporation of water and subsequent aggregation of particles at 350^{o} C as evident from FTIR results where the water absorbance band in the case of E3 nanoparticles is less deeper as compared to water absorbance band in T, E1 and E2 particles. Similar results were observed by George et al. (2020) where they found that at the maximum calcination temperatures the size of nanoparticles decreased. The other reason behind this may be the inherent properties of the nanoparticles, in which particles always tend to acquire stable shape and size at particular conditions as reported by Malviya et al. (2015). The reason for the increase in the size of E1

particles compared to the size of T particles in HRTEM analysis which is opposite to XRD analysis can be attributed to the increased growth rate at 70^{o}C temperature, the similar results have been found in the study of Hongyu *et al*. (2020). From FESEM and HRTEM analysis it can be concluded that with the increase in temperature at constant incubation duration size of CuONPs increases and particles tends to take a stable shape with smooth boundaries.

Toxicity evaluation of all types of CuONPs (T, E1, E2, and E3) on granulosa cells showed that all these types of nanoparticles exhibited toxicity and triggered an increase in the percentage of pre-apoptotic and apoptotic cells after 24 hrs. of exposure duration. Our results support the earlier findings of Fatahian-Dehkordi et al. (2017). This CuONPs cytotoxicity can be attribute to presence of Cu^{2+} released by the CuONPs in culture media as reported by El Bialy et al. (2020) and Katsumiti et al (2018). Cu^{2+} on reacting with cells caused increased ROS thus damaged DNA. The significant higher toxicity due to CuONPs at higher doses, when compared to control, can possibly be due to an increase in the concentration of nanoparticleslead to increased amount of Cu^{2+} ions released by CuONPs in the medium (Wongrakpanich et al. 2016).

Along with this, it was also observed that only T nanoparticles at higher doses showed significant differences in the number of apoptotic cells when compared to control and lower doses of E1, E2, and E3 nanoparticles. The difference in size can be the reason behind significant toxicity of T nanoparticles at higher doses compared to lower doses of other nanoparticles. Kim et al. (2012) reported the similar results where small sized nanoparticles reported more toxicity than large size nanoparticles. Whereas, the Significance of higher toxicity that was seen in both doses of T nanoparticles in healthy cells and non-significant toxicity in the case of lower doses of E3 nanoparticles in pre-apoptotic cells when compared to control can be attributed to change in the shape of nanoparticles. Reason for this toxicity may be the rate of release of Cu^{2+} by different shapes of particles. As reported by Wongrakpanich et al. (2016) and Misra et al. (2014) the rate of release of Cu^{2+} in the case of spherical nanoparticles were more as compared to other shapes of particles. Misra et al. (2014) specifically reported the reason for this higher release of Cu^{2+} and concluded that spherical CuONPs has highest specific surface area (SSA) as compared to the rod and spindle-shaped CuO nanoparticles. Thus we can also deduce here that capsule-shaped particles seem to have lesser SSA than spherical nanoparticles and needle-shaped nanoparticles, so the release of Cu^{2+} from capsule-shaped CuONPs is slower and hence at lower doses (10 µg ml^{-1}) the cytotoxicity caused by this type of nanoparticles is also less, hence it causes less toxicity.

The mechanism behind CuONPs toxicity is yet not confirmed but an increase in oxidative stress seems to be the main reason as reported by Fahmy and Cormier (2009) and Berntsen et al. (2010) where increased oxidation stress was reported in cells cultured with CuONPs. Ahamed et al. (2010) also reported similar results where nanoparticles could cause an increase in levels of lipid peroxidation and ROS production while lowering the levels of antioxidants. Cytotoxicity of the CuONPs may be due to DNA damaging capabilities of CuONPs as Akhtar et al. (2016) and Thit et al. (2015) reported that CuONPs can cause genotoxic effects either directly associating with DNA or indirectly by activating phagocytes and

macrophages. Time of CuONPs exposure to the cells might have played some role in the toxicity as Misra et al. (2014) reported that the rate of dissolution of spherical nanoparticles is quicker than the rate of dissolution of other shapes of particles. Thus, cells got exposed to the Cu^{2+} to a greater extent in case of spherical particles than other shaped particles.

Conclusion

In the present study, we have synthesized the CuO nanoparticles at different incubation temperatures (70^{o}C, 150^{o}C, and 350^{o}C). XRD at different angles showed that all the particles were monoclinic crystal structures. FTIR absorbance showed that all the particles have CuO stretching. FESEM and HRTEM showed that temperature has a significant impact on the shape of nanoparticles. With the increase in temperature shape of nanoparticles increased and had regular boundaries. While there are many studies providing insight on the toxicity of nanoparticles caused due to their size and surface chemistry, but scattered information is available about shape-related nanoparticle toxicity. The present research suggests that shape has a significant impact on the cytotoxicity of the nanoparticles. In this study, spherical particles proved to be more toxic as compared to needle and capsule-shaped particles. Our study provides the scope for further research to analyze the nanoparticles induced toxicity due to variation in shape besides size and surface chemistry differences.

Declarations

Ethics approval and consent to participate

Not applicable

Consent for publication

Not applicable

Availability of data and materials

The datasets used and/or analysed during the current study are available from the

corresponding author on reasonable request.

Competing interests

The authors declare that they have no competing interests.

Funding

The necessary funding for the work was provided by Council of Science and Industrial Research (CSIR) in the form of Senior Research Fellowship (SRF) with file no. 09/105(0277)/2018-EMR-I to one of the author (Mr. Chetan Kumar).

Author contribution Rajnesh Kumar Sharma: Conceptualization, Validation, Investigation, Resources, Proof Reading- Review and editing, Supervision.

Chetan Kumar: Conceptualization, Resources, Writing-Original draft, Visualization, Funding acquisition.

Acknowledgement

The authors are grateful to the Council of Science and Industrial Research (CSIR) for the financial support granted as Senior Research Fellowship (SRF) with file no. 09/105(0277)/2018-EMR-I to Mr. Chetan Kumar. We are also thankful to the Department of Zoology, Kurukshetra University, Kurukshetra (India) for UGC-SAP sponsored laboratory facilities.

References

1. Ahamed M, Siddiqui MA, Akhtar MJ, Ahmad I, Pant AB Alhadlaq HA (2010) Genotoxic potential of copper oxide nanoparticles in human lung epithelial cells. Biochemical and biophysical research communications, 396(2):578-583
2. Ahamed M, Alhadlaq HA, Khan MA, Karuppiah P, Al-Dhabi NA (2014) Synthesis, characterization, and antimicrobial activity of copper oxide nanoparticles. Journal of Nanomaterials 2014
3. Akhtar MJ, Kumar S, Alhadlaq HA, Alrokayan SA, Abu-Salah KM, Ahamed M (2016) Dose-dependent genotoxicity of copper oxide nanoparticles stimulated by reactive oxygen species in human lung epithelial cells. Toxicology and industrial health 32(5):809-821
4. Araújo VR, Lima-Verde IB, Báo SN, Campello CC, Silva JR, Rodrigues AP, Figueiredo JR (2010) Bone morphogenetic protein-6 (BMP-6) induces atresia in goat primordial follicles cultured in vitro. Pesquisa Veterinária Brasileira Sep;30(9):770-81.
5. Arun KJ, Batra AK, Krishna A, Bhat K, Aggarwal MD, Francis PJ (2015) Surfactant free hydrothermal synthesis of copper oxide nanoparticles. Am. J. Mater. Sci 5:36-8.
6. Aruoja V, Dubourguier HC, Kasemets K, Kahru A (2009) Toxicity of nanoparticles of CuO, ZnO and TiO2 to microalgae Pseudokirchneriella subcapitata. Science of the total environment Feb 1;407(4):1461-8.
7. Bahadar H, Maqbool F, Niaz K, Abdollahi M (2016) Toxicity of nanoparticles and an overview of current experimental models. Iranian biomedical journal Jan;20(1):1.
8. Berntsen P, Park CY, Rothen-Rutishauser B, Tsuda A, Sager TM, Molina RM, Donaghey TC, Alencar AM, Kasahara DI, Ericsson T, Millet EJ (2010) Biomechanical effects of environmental and engineered particles on human airway smooth muscle cells. Journal of the Royal Society Interface Jun 6;7(suppl_3):S331-40.
9. Braydich-Stolle L, Hussain S, Schlager JJ, Hofmann MC (2005) In vitro cytotoxicity of nanoparticles in mammalian germline stem cells. Toxicological sciences Dec 1;88(2):412-9.
10. Broaddus VC, Yang L, Scavo LM, Ernst JD, Boylan AM (1996) Asbestos induces apoptosis of human and rabbit pleural mesothelial cells via reactive oxygen species. The Journal of clinical investigation

Nov 1;98(9):2050-9.

11. Buzea C, Pacheco II, Robbie K (2007) Nanomaterials and nanoparticles: sources and toxicity. Biointerphases Dec 28;2(4):MR17-71.
12. Carbone MC, Tatone C, Monache SD, Marci R, Caserta D, Colonna R, Amicarelli F (2003) Antioxidant enzymatic defences in human follicular fluid: characterization and age-dependent changes. MHR: Basic science of reproductive medicine Nov;9(11):639-43.
13. Cardeilhac PT, Whitaker BR (1988) Copper treatments: uses and precautions. Veterinary Clinics of North America: Small Animal Practice Mar 1;18(2):435-48.
14. Chavany C, Saison-Behmoaras T, Le Doan T, Puisieux F, Couvreur P, Hélène C (1994) Adsorption of oligonucleotides onto polyisohexylcyanoacrylate nanoparticles protects them against nucleases and increases their cellular uptake. Pharmaceutical research Sep;11(9):1370-8.
15. Chawla JS, Amiji MM (2002) Biodegradable poly (ε-caprolactone) nanoparticles for tumor-targeted delivery of tamoxifen. International journal of pharmaceutics Dec 5;249(1-2):127-38.
16. Chopra R, Kashyap N, Kumar A, Banerjee D (2020) Chemical Synthesis of Copper Oxide Nanoparticles Study of its Optical and Electrical Properties. Int. J. Eng. Res Technol..;9:258-61.
17. Cohu CM, Pilon M (2010) Cell biology of copper. In: Cell biology of metals and nutrients, Springer, Berlin, Heidelberg pp. 55-74
18. El Bialy BE, Hamouda RA, Abd Eldaim MA, El Ballal SS, Heikal HS, Khalifa HK, Hozzein WN (2020) Comparative Toxicological Effects of Biologically and Chemically Synthesized Copper Oxide Nanoparticles on Mice. International Journal of Nanomedicine 15:3827.
19. Fahmy B, Cormier SA (2009) Copper oxide nanoparticles induce oxidative stress and cytotoxicity in airway epithelial cells. Toxicology In Vitro Oct 1;23(7):1365-71.
20. Fatahian-Dehkordi R, Reaisi M, Heidarnejad MS, Mohebbi A (2017) Serum biochemical status and morphological changes in mice ovary associated with copper oxide nanoparticles after thiamine therapy. Journal of Herbmed Pharmacology 6.
21. Ficai D, Grumezescu AM (2017) Nanostructures for novel therapy: synthesis, characterization and applications. Elsevier Feb 25.
22. Franklin NM, Rogers NJ, Apte SC, Batley GE, Gadd GE, Casey PS (2007) Comparative toxicity of nanoparticulate ZnO, bulk ZnO, and ZnCl2 to a freshwater microalga (Pseudokirchneriella subcapitata): the importance of particle solubility. Environmental science & technology Dec 15;41(24):8484-90.
23. Gawande MB, Goswami A, Felpin FX, Asefa T, Huang X, Silva R, Zou X, Zboril R, Varma RS (2016) Cu and Cu-based nanoparticles: synthesis and applications in catalysis. Chemical reviews Mar 23;116(6):3722-811.
24. George A, Raj DM, Raj AD, Irudayaraj AA, Arumugam J, Prabu HJ, Sundaram SJ, Al-Dhabi NA, Arasu MV, Maaza M, Kaviyarasu K (2020) Temperature effect on CuO nanoparticles: Antimicrobial activity towards bacterial strains. Surfaces and Interfaces Dec 1;21:100761.

25. Gerber C, Lang HP (2006) How the doors to the nanoworld were opened. Nature nanotechnology Oct;1(1):3-5.
26. Gratton SE, Ropp PA, Pohlhaus PD, Luft JC, Madden VJ, Napier ME, DeSimone JM (2008) The effect of particle design on cellular internalization pathways. Proceedings of the National Academy of Sciences Aug 19;105(33):11613-8.
27. Hill EK, Li J (2017) Current and future prospects for nanotechnology in animal production. Journal of animal science and biotechnology Dec;8(1):1-3.
28. Liu H, Zhang H, Wang J, Wei J (2020) Effect of temperature on the size of biosynthesized silver nanoparticle: deep insight into microscopic kinetics analysis. Arabian Journal of Chemistry Jan 1;13(1):1011-9.
29. Huang X, Teng X, Chen D, Tang F, He J (2010) The effect of the shape of mesoporous silica nanoparticles on cellular uptake and cell function. Biomaterials Jan 1;31(3):438-48.
30. Ingale AG, Chaudhari AN (2013) Biogenic synthesis of nanoparticles and potential applications: an eco-friendly approach. J Nanomed Nanotechol ;4(165):1-7.
31. Karlsson HL, Cronholm P, Gustafsson J, Moller L (2008) Copper oxide nanoparticles are highly toxic: a comparison between metal oxide nanoparticles and carbon nanotubes. Chemical research in toxicology Sep 15;21(9):1726-32.
32. Katsumiti A, Thorley AJ, Arostegui I, Reip P, Valsami-Jones E, Tetley TD, Cajaraville MP (2018) Cytotoxicity and cellular mechanisms of toxicity of CuO NPs in mussel cells in vitro and comparative sensitivity with human cells. Toxicology in Vitro Apr 1;48:146-58.
33. Khan HU, Tariq M, Shah M, Jan MT, Iqbal M, Khan J, Ahsan AR, Rahim A (2020) The efficacy of polyvinylpyrrolidone (PVP)/CuO nanocomposite as an appropriate room temperature humidity sensing material: fabrication of highly sensitive capacitive resistive type humidity sensor. Journal of Materials Science: Materials in Electronics May;31(10):7698-707.
34. Kim TH, Kim M, Park HS, Shin US, Gong MS, Kim HW (2012) Size-dependent cellular toxicity of silver nanoparticles. Journal of biomedical materials research Part A Apr;100(4):1033-43.
35. Kulkarni SK, Kulkarni SK (2015) Nanotechnology: principles and practices. Springer
36. Lanone S, Rogerieux F, Geys J, Dupont A, Maillot-Marechal E, Boczkowski J, Lacroix G, Hoet P (2009) Comparative toxicity of 24 manufactured nanoparticles in human alveolar epithelial and macrophage cell lines. Particle and fibre toxicology Dec;6(1):1-2.
37. Lima-Verde IB, Matos MH, Celestino JJ, Rossetto R, Báo SN, Campello CC, Figueiredo JR (2012) Progesterone and Follicle Stimulating Hormone interact and promote goat preantral follicles survival and development in vitro. Pesquisa Veterinária Brasileira Apr;32(4):361-7.
38. Liu S, Xia T (2020) Continued Efforts on Nanomaterial-Environmental Health and Safety Is Critical to Maintain Sustainable Growth of Nanoindustry. Small May;16(21):2000603.
39. Liu J, Sonshine DA, Shervani S, Hurt RH (2010) Controlled release of biologically active silver from nanosilver surfaces. ACS nano Nov 23;4(11):6903-13.

40. Liu X, Qin D, Cui Y, Chen L, Li H, Chen Z, Gao L, Li Y, Liu J (2010) The effect of calcium phosphate nanoparticles on hormone production and apoptosis in human granulosa cells. Reproductive Biology and Endocrinology Dec;8(1):1-8.
41. Malviya N, Carpenter G, Oswal N, Gupta N (2015) Synthesis and characterization of CuO nano particles using precipitation method. In: AIP Conference Proceedings Jun 24;1665(1):050038 AIP Publishing LLC.
42. Misra SK, Nuseibeh S, Dybowska A, Berhanu D, Tetley TD, Valsami-Jones E (2014) Comparative study using spheres, rods and spindle-shaped nanoplatelets on dispersion stability, dissolution and toxicity of CuO nanomaterials. Nanotoxicology Jun 1;8(4):422-32.
43. Moghimi SM, Hunter AC, Murray JC (2001) Long-circulating and target-specific nanoparticles: theory to practice. Pharmacological reviews Jun 1;53(2):283-318.
44. Na HB, Song IC, Hyeon T (2009) Inorganic nanoparticles for MRI contrast agents. Advanced materials Jun 5;21(21):2133-48.
45. Pal DB, Giri DD, Bhargav M, Singh P, Mishra PK (2015) Synthesis and characterization of CuO nanoparticles by aqueous precipitation method. In: International Conference on Nanotechnology.
46. Panyam J, Labhasetwar V (2003) Biodegradable nanoparticles for drug and gene delivery to cells and tissue. Advanced drug delivery reviews Feb 24;55(3):329-47.
47. Piret JP, Jacques D, Audinot JN, Mejia J, Boilan E, Noël F, Fransolet M, Demazy C, Lucas S, Saout C, Toussaint O (2012) Copper (II) oxide nanoparticles penetrate into HepG2 cells, exert cytotoxicity via oxidative stress and induce pro-inflammatory response. Nanoscale 4(22):7168-84.
48. Richardson HW (1997) Handbook of copper compounds and applications. CRC Press
49. Santos HB, Sato Y, Moro L, Bazzoli N, Rizzo E (2008) Relationship among follicular apoptosis, integrin β 1 and collagen type IV during early ovarian regression in the teleost Prochilodus argenteus after induced spawning. Cell and tissue research Apr;332(1):159-70.
50. Sedaghat Z, Taghavinia N, Marandi M (2006) Thermal control of the size and crystalline phase of CdS nanoparticles. Nanotechnology Jul 6;17(15):3812.
51. Sharma RK, Bhardwaj JK (2009) Ultrastructural characterization of apoptotic granulosa cells in caprine ovary. Journal of microscopy Dec;236(3):236-42.
52. Sharma RK (2000) Follicular atresia in goat: A review. Indian Journal of Animal Sciences Oct 1;70(10):1035-46.
53. Siddiqui S, Goddard RH, Bielmyer-Fraser GK (2015) Comparative effects of dissolved copper and copper oxide nanoparticle exposure to the sea anemone, Exaiptasia pallida. Aquatic Toxicology Mar 1;160:205-13.
54. Stelzer R, Hutz RJ (2009) Gold nanoparticles enter rat ovarian granulosa cells and subcellular organelles, and alter in-vitro estrogen accumulation. Journal of Reproduction and Development 0909170201-.

55. Studer AM, Limbach LK, Van Duc L, Krumeich F, Athanassiou EK, Gerber LC, Moch H, Stark WJ (2010) Nanoparticle cytotoxicity depends on intracellular solubility: comparison of stabilized copper metal and degradable copper oxide nanoparticles Toxicology letters. Sep 1;197(3):169-74.
56. Sun J, Wang S, Zhao D, Hun FH, Weng L, Liu H (2011) Cytotoxicity, permeability, and inflammation of metal oxide nanoparticles in human cardiac microvascular endothelial cells. Cell biology and toxicology Oct 1;27(5):333-42.
57. Taghavi SM, Momenpour M, Azarian M, Ahmadian M, Souri F, Taghavi SA, Sadeghain M, Karchani M (2013) Effects of nanoparticles on the environment and outdoor workplaces. Electronic physician Oct;5(4):706.
58. Tamilvanan A, Balamurugan K, Ponappa K, Kumar BM (2014) Copper nanoparticles: synthetic strategies, properties and multifunctional application. International Journal of Nanoscience Apr 20;13(02):1430001.
59. Tang S, Wang M, Germ KE, Du HM, Sun WJ, Gao WM, Mayer GD (2015) Health implications of engineered nanoparticles in infants and children. World Journal of Pediatrics Aug;11(3):197-206.
60. Thit A, Selck H, Bjerregaard HF (2015) Toxic mechanisms of copper oxide nanoparticles in epithelial kidney cells. Toxicology in vitro 2015 Aug 1;29(5):1053-9.
61. Tortora GJ, Derrickson BH (2018) Principles of anatomy and physiology. John Wiley & Sons; May 15.
62. Venkataraman S, Hedrick JL, Ong ZY, Yang C, Ee PL, Hammond PT, Yang YY (2011) The effects of polymeric nanostructure shape on drug delivery. Advanced drug delivery reviews Nov 1;63(14-15):1228-46.
63. Vidyasagar CC, Naik YA, Venkatesha TG, Viswanatha R (2012) Solid-state synthesis and effect of temperature on optical properties of CuO nanoparticles. Nano-Micro Letters Jun 1;4(2):73-7.
64. Wang Y, Aker WG, Hwang HM, Yedjou CG, Yu H, Tchounwou PB (2011) A study of the mechanism of in vitro cytotoxicity of metal oxide nanoparticles using catfish primary hepatocytes and human HepG2 cells. Science of the total environment Oct 15;409(22):4753-62.
65. Wongrakpanich A, Mudunkotuwa IA, Geary SM, Morris AS, Mapuskar KA, Spitz DR, Grassian VH, Salem AK (2016) Size-dependent cytotoxicity of copper oxide nanoparticles in lung epithelial cells. Environmental Science: Nano 3(2):365-74.
66. Xu J, Li Z, Xu P, Xiao L, Yang Z (2013) Nanosized copper oxide induces apoptosis through oxidative stress in podocytes. Archives of toxicology Jun 1;87(6):1067-73.
67. Yu M, Mo Y, Wan R, Chien S, Zhang X, Zhang Q (2010) Regulation of plasminogen activator inhibitor-1 expression in endothelial cells with exposure to metal nanoparticles. Toxicology letters May 19;195(1):82-9.
68. Yu YS, Sui HS, Han ZB, Wei LI, Luo MJ, Tan JH (2004) Apoptosis in granulosa cells during follicular atresia: relationship with steroids and insulin-like growth factors. Cell research Aug;14(4):341-6.

Tables

Table 1 Division of particles into groups and their respective incubation conditions

GROUPS	INCUBATION CONDITIONS
T	70°C for 5 hrs.
E_1	T + 70°C for 5 hrs.
E_2	T + 150°C for 5 hrs.
E_3	T + 350°C for 5 hrs.

Table 2 Absorbance band of CuONPs incubated at incubation conditions and their related absorbance range and respective functional groups.

Nanoparticles	FTIR SPECTRA (cm^{-1})	FUNCTIONAL GROUP
T	516 and 602	CuO
	1382 and 1633	Carbonyl group bidentate ligand formation with CuO
	2921	$-CH_2-$
	3426	-OH
E_1	516 and 599	CuO
	1385 and 1633	Carbonyl group bidentate ligand formation with CuO
	2922	$-CH_2-$
	3425	-OH
E_2	499 and 600	CuO
	1385 and 1630	Carbonyl group bidentate ligand formation with CuO
	2920	$-CH_2-$
	3417	-OH
E_3	512 and 600	CuO
	1384 and 1634	Carbonyl group bidentate ligand formation with CuO
	2921	$-CH_2-$
	3354	-OH

Table 3 Number of healthy, pre-apoptotic and apoptotic cells of all treatment groups. Data represent the Mean ± Standard Error of Mean.

Treatments		Healthy	Pre-Apoptotic	Apoptotic
Control		11.73 ± 1.76^{c}	$0.73 \pm .195^{a}$	1.18 ± 0.352^{a}
T Particles	10 µg ml^{-1}	7.36 ± 0.678^{ab}	2.91 ± 0.392^{bc}	3.36 ± 0.544^{abc}
	20 µg ml^{-1}	4.27 ± 0.428^{a}	4.45 ± 0.511^{c}	4.91 ± 0.756^{c}
E1 Particles	10 µg ml^{-1}	8.18 ± 0.444^{bc}	3.00 ± 0.618^{bc}	2.45 ± 0.455^{ab}
	20 µg ml^{-1}	6.27 ± 0.557^{ab}	3.27 ± 0.304^{bc}	4.09 ± 0.579^{bc}
E2 Particles	10 µg ml^{-1}	8.45 ± 0.743^{bc}	2.91 ± 0.476^{bc}	2.27 ± 0.384^{ab}
	20 µg ml^{-1}	6.73 ± 0.662^{ab}	3.27 ± 0.304^{bc}	3.64 ± 0.491^{bc}
E3 Particles	10 µg ml^{-1}	9.36 ± 0.823^{bc}	2.45 ± 0.366^{ab}	1.82 ± 0.325^{ab}
	20 µg ml^{-1}	6.82 ± 0.882^{ab}	3.00 ± 0.447^{bc}	3.82 ± 0.553^{bc}

values are expressed as mean±sem. anova with tukey post hoc test was used for analysis; different letters indicate significant differences among means of treatment at each duration ($p<0.05$) after tukey's test. ao: acridine orange

Figures

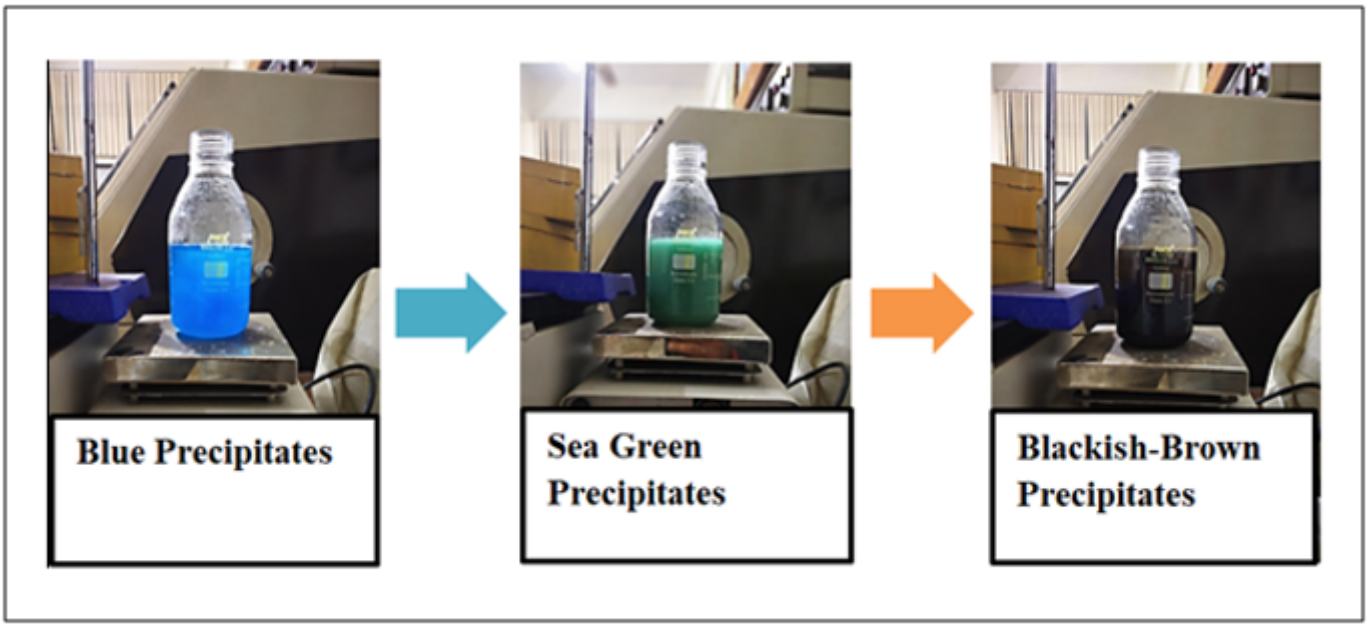

Figure 1

Process Synthesis of CuONPs color confirmation.

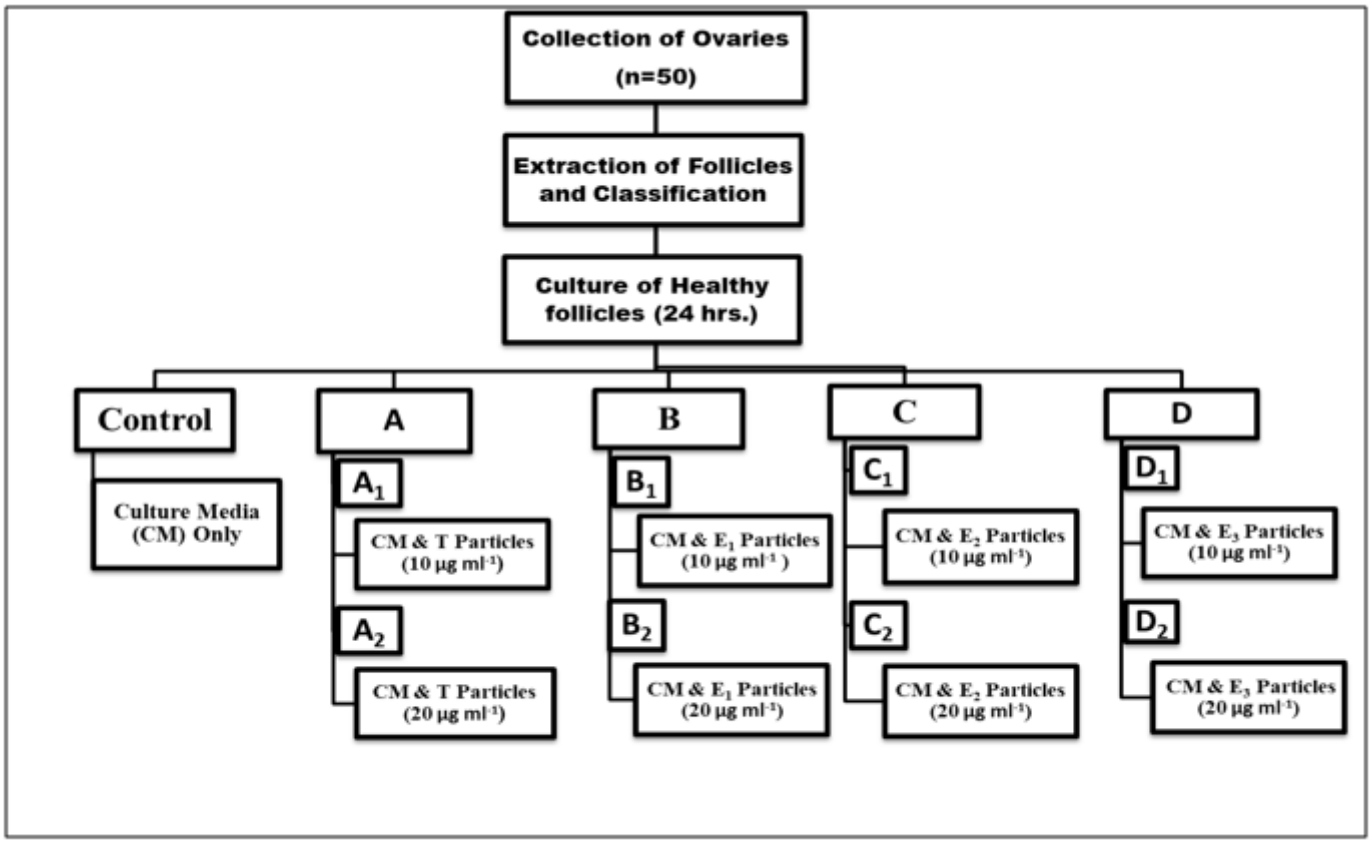

Figure 2

Experimental layout for in vitro follicular culture of goat ovaries.

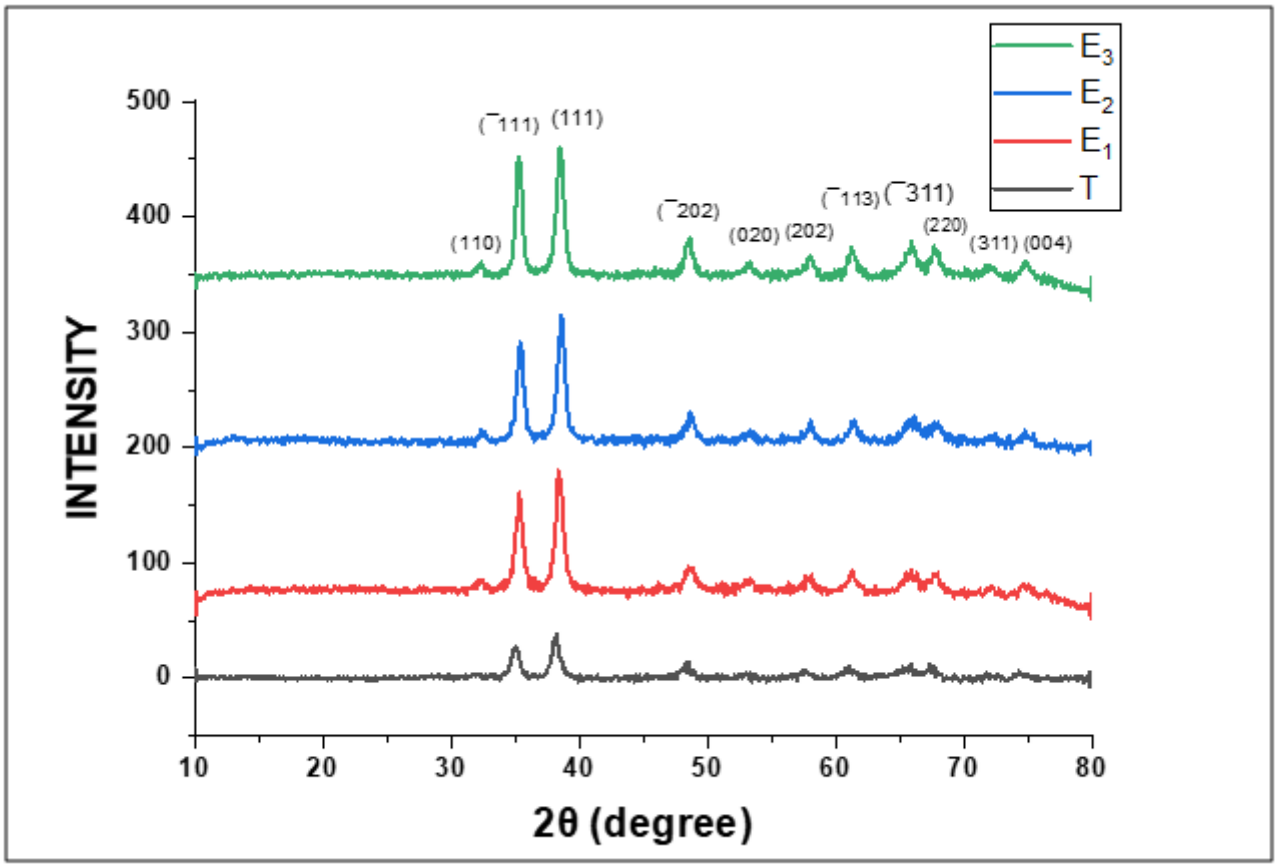

Figure 3

X-Ray Diffraction of CuO nanoparticles at various incubation conditions.

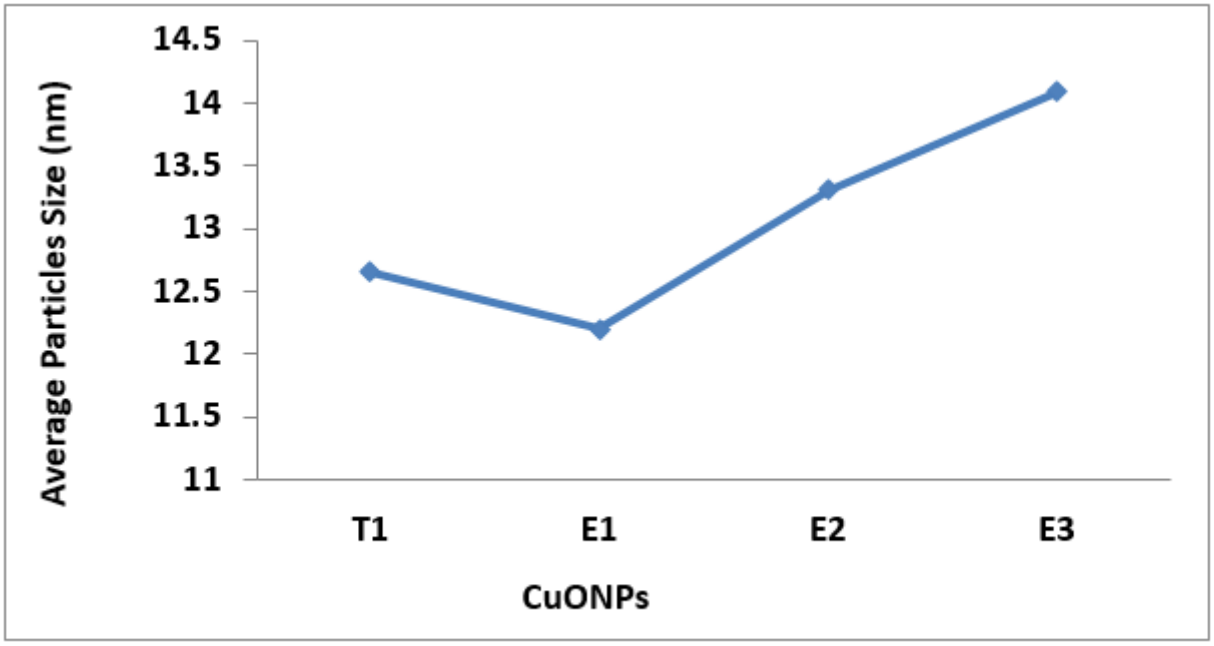

Figure 4

Relationship between CuONPs incubated at different conditions and average crystalline size.

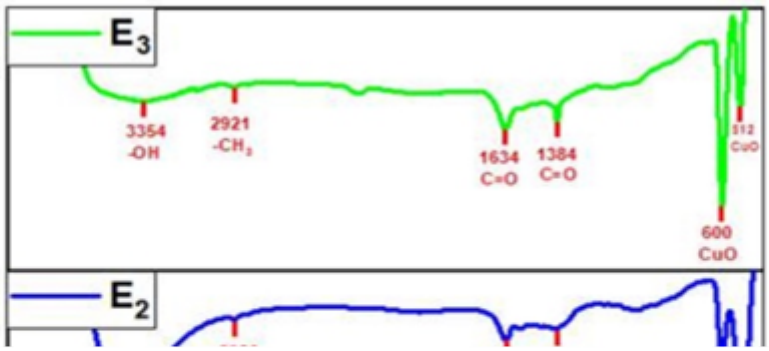

Figure 5

FTIR spectrum of CuO nanoparticles incubated at various conditions.

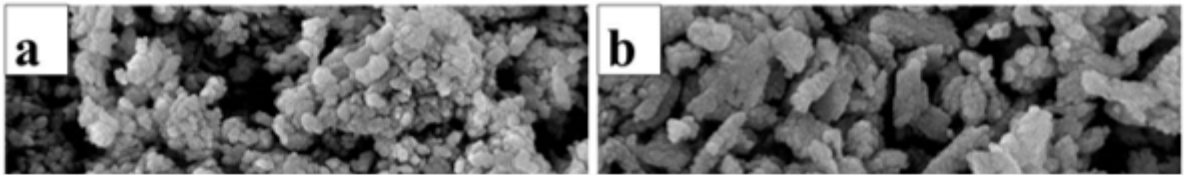

Figure 6

FESEM images of different CuONPs (500 nm). (a) T CuONPs (b) E1 CuONPs (c) E2 CuONPs (d) E3 CuONPs.

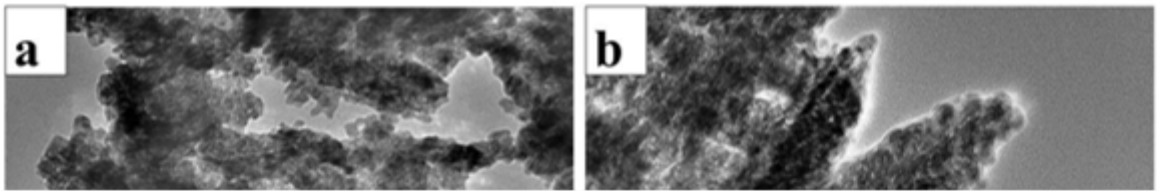

Figure 7

High Resolution Transmission Electron Microscopy images of different CuONPs (a) T CuONPs, (b) E1 CuONPs, (c) E2 CuONPs and (d) E3 CuONPs.

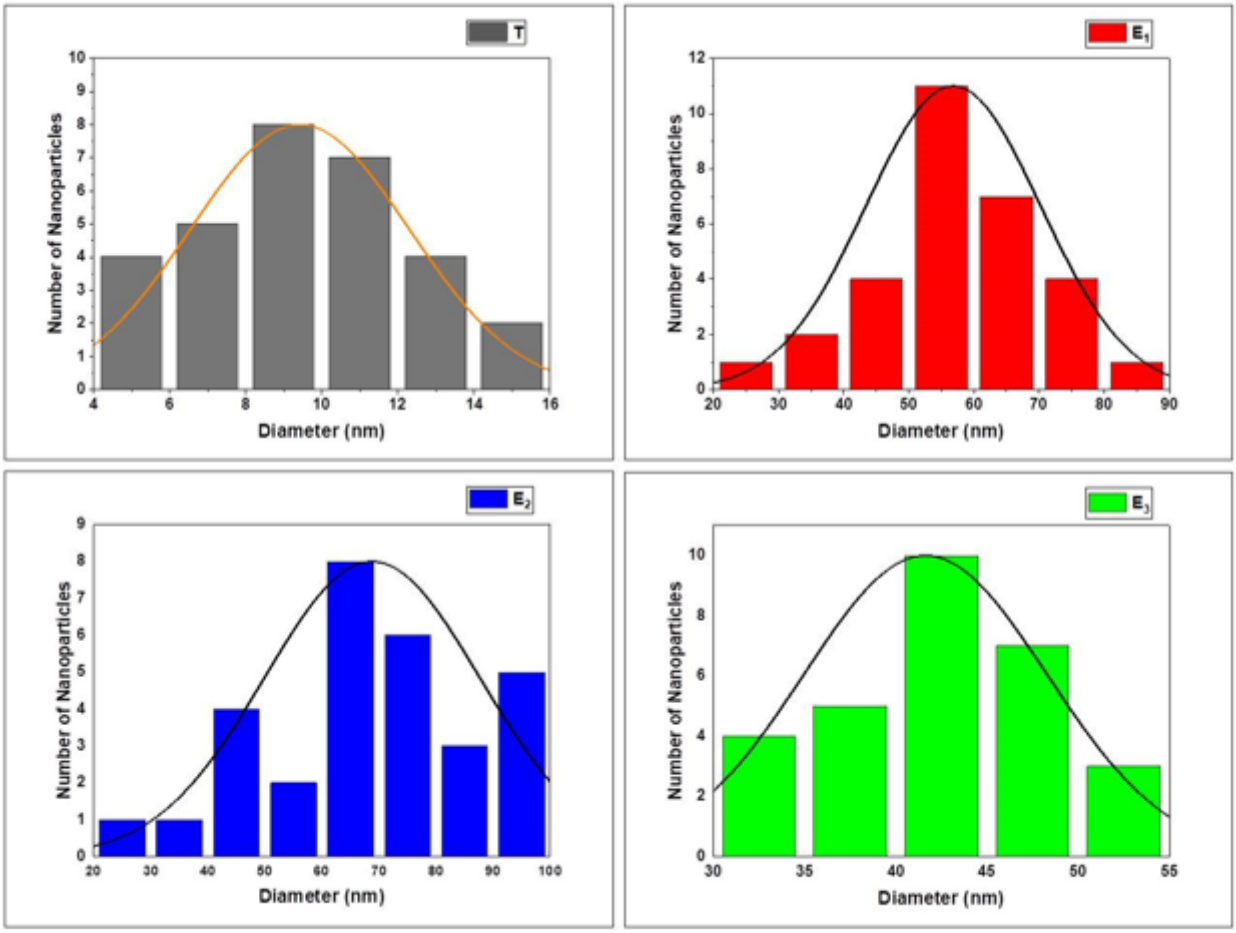

Figure 8

Histograms of CuONPs formed at different incubation conditions

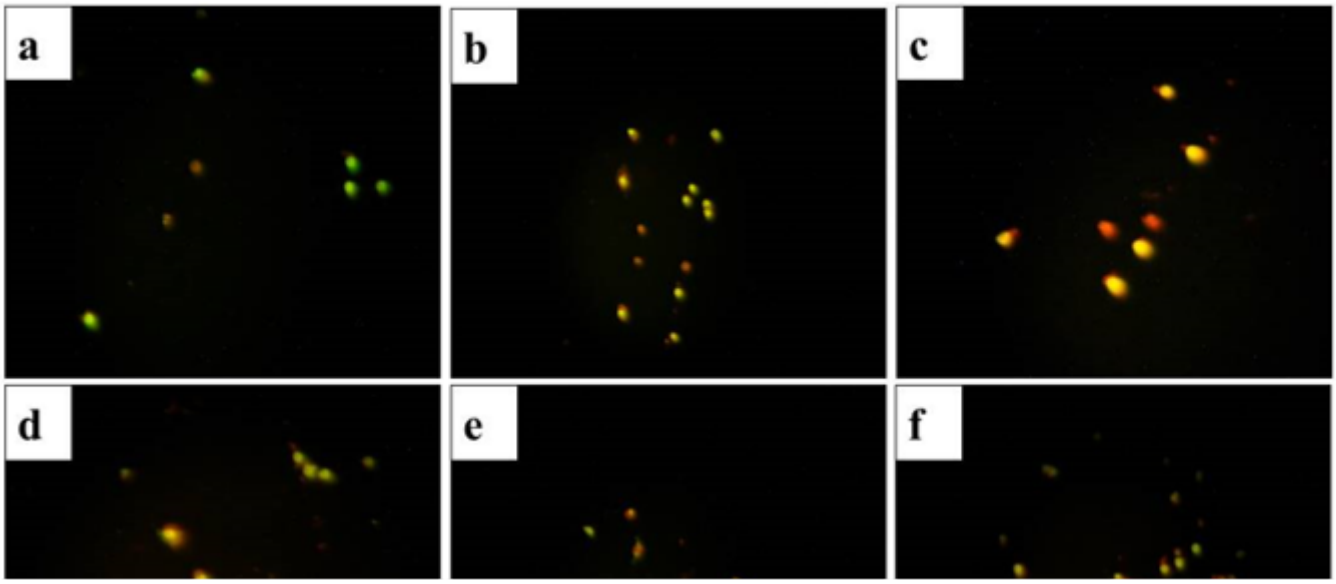

Figure 9

Fluorescent microscopic images of the granulosa cells of ovarian antral follicles treated with Cupric Oxide Nanoparticles (CuONPs) at 10 µg ml-1 and 20 µg ml-1 by T nanoparticles (b, c), E1 (d, e), E2 (f, g), and E3 (h, i) nanoparticles in comparison to control (a) stained with AO depicting apoptotic cells as red and pre-apoptotic cells as yellow/yellowish red and healthy cells as green after 24 hrs. cultural duration at X400.

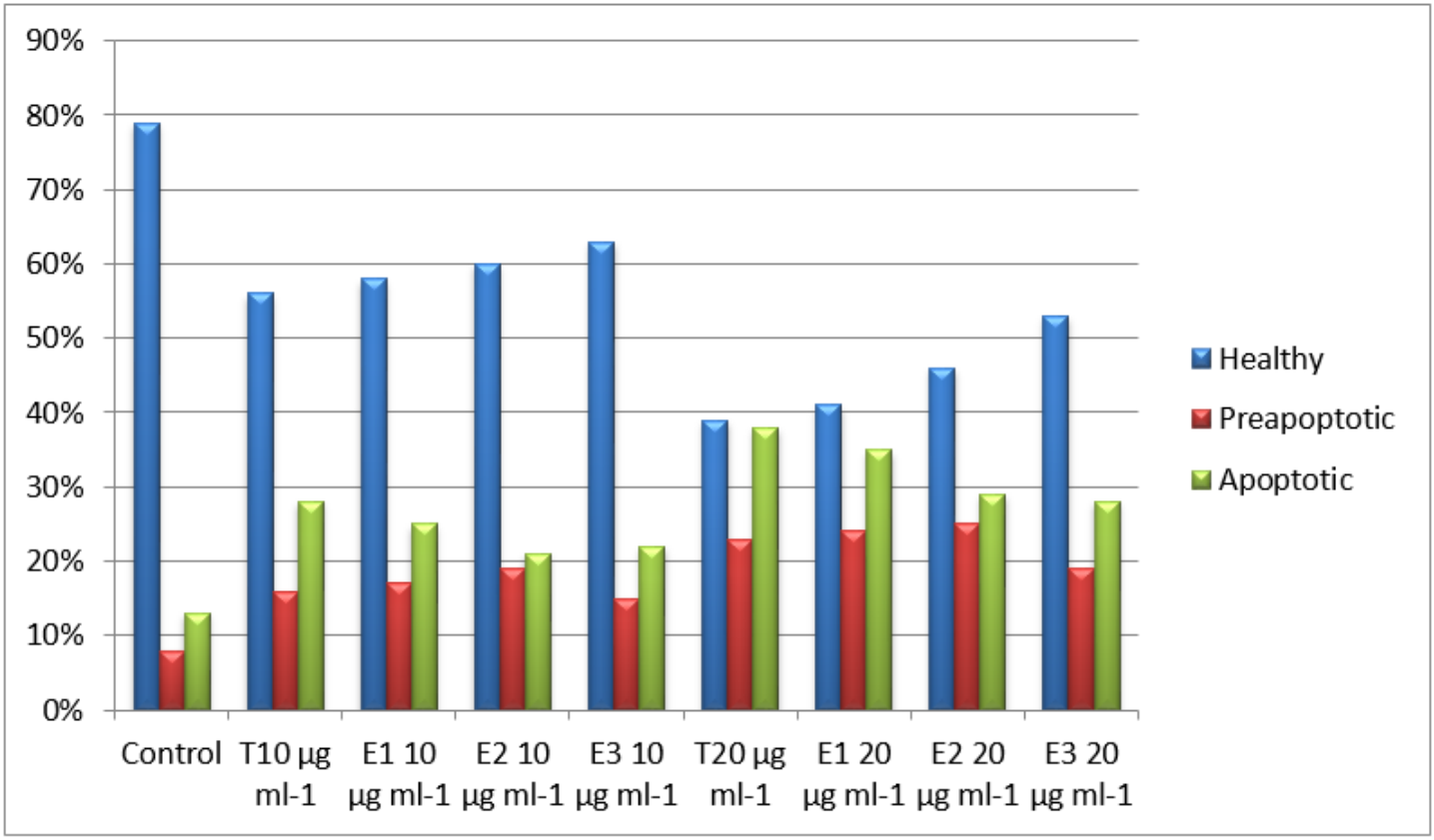

Figure 10

Apoptotic Percentage Index of granulosa cells treated with CuONPs incubated at different conditions at 10 µg ml-1 and 20 µg ml-1 doses for 24 hrs.

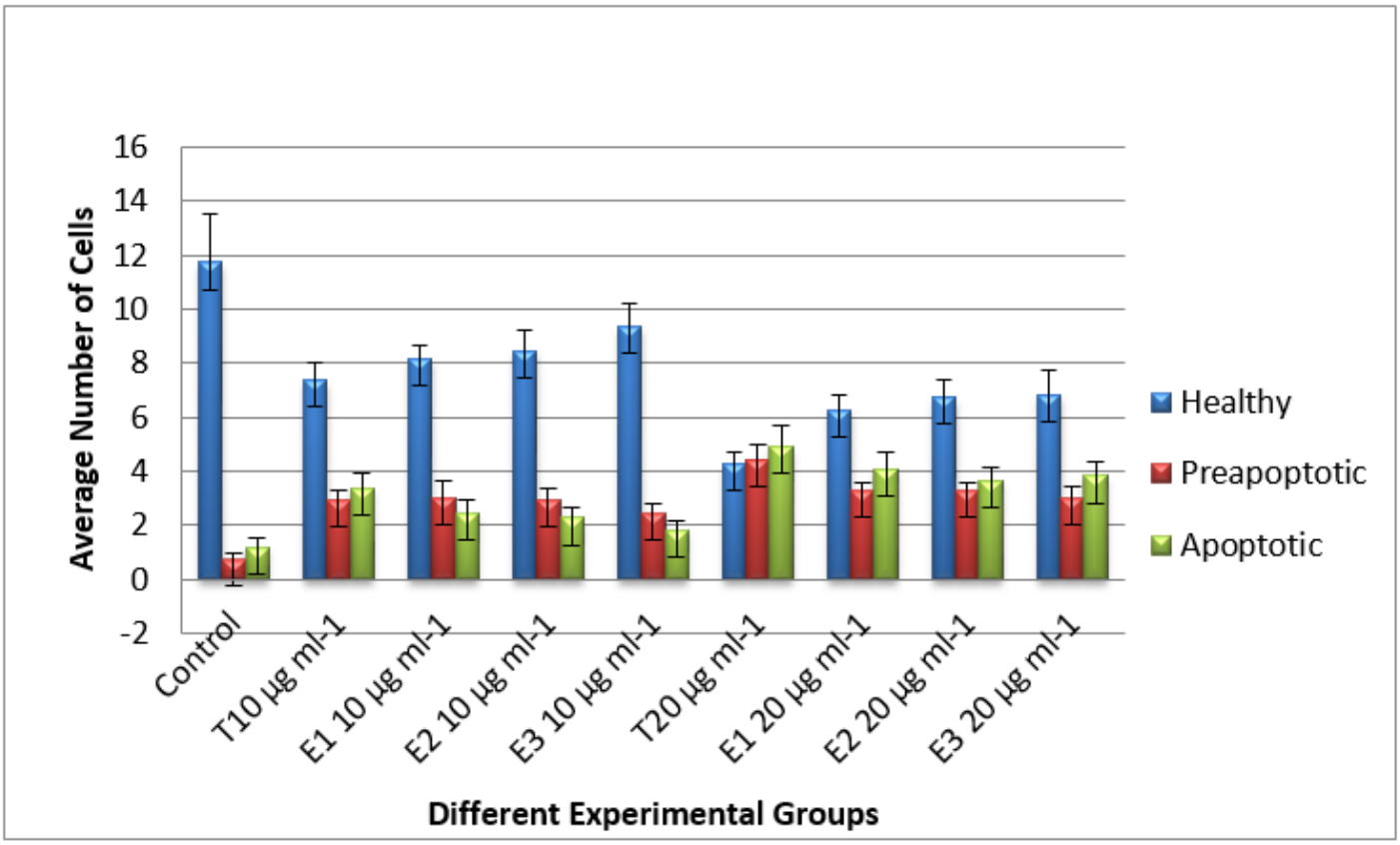

Figure 11

Cytotoxicity of CuONPs as determined by using granulosa cells, treated with T, E1, E2 and E3 nnaoparticles for 24 hrs. of cultural duration. Data represent the Mean ± Standard Error of Mean.